Multi-scale design of ionic liquid solvents and capture processes for high-pressure CO_2 point sources

Kyeongjun Seo, Joan F. Brennecke, Thomas F. Edgar, Mark A. Stadtherr, and Michael Baldea*

McKetta Department of Chemical Engineering, University of Texas at Austin, Austin, TX 78712, United States

E-mail: mbaldea@che.utexas.edu

Abstract

We introduce a multi-scale modeling and optimization framework for integrated process and molecular design of carbon capture systems from point sources. We focus on using ionic liquid (IL)-based solvents, which have been proposed as environmentally benign and effective solvents for carbon capture. The thermophysical properties of the capture solvent are described using perturbed-chain statistical associating fluid theory (PC-SAFT) with a set of continuous molecular descriptors. At the macroscopic level, detailed and rigorous correlations are used for characterizing mass and heat transfer. The optimization of the resulting multi-scale flowsheet model aims to minimize total annualized cost, and is performed using pseudo-transient methods. An extensive case study considers a broad repertoire of point-source carbon capture scenarios (in terms of source characteristics and capture rate), proving the superiority of simultaneously and holistically designing the process and the solvent, relative to existing results that rely on a single, fixed solvent.

Introduction

Mitigating carbon emissions from point sources related to power generation and manufacturing is a key element of addressing global warming. On the one hand, fossil-fueled power plants are anticipated to remain in use for several decades to provide grid resiliency

while grid-level energy storage is widely developed. On the other hand, carbon capture and sequestration is essential for industrial decarbonization, given that technology and efficiency advances alone cannot completely eliminate emissions from manufacturing.[1]

Significant progress has been made on solvent-based carbon capture technologies for point sources, using second generation amine solvents such as piperazine[2,3] and, more recently, ionic liquids[4,5] and other water-lean solvents.[6,7] Given the vastness of the application space (point sources of CO_2 differ widely in terms of, e.g., flow rate, concentration of CO_2, moisture content, and levels of other criteria pollutants) there is no "one size fits all" capture solution. In this context, the reduction to practice of carbon capture technologies typically amounts to tailoring a technology based on an established solvent to a specific application. This effort is referred to as "process design" and entails selecting the size of equipment (such as height and diameter of unit operations) and operating parameters (such as pressures, temperatures, and solvent flow rates) for a processing facility that follows the general configuration shown in Figure 1. The objective of this selection process is to maximize the efficiency of the facility for the particular application or source type; equivalently, one aims to lower the energy spent and, ultimately the cost (including capital and operating expenses) per unit mass of CO_2 captured for each case.

This approach ignores an important additional set of degrees of freedom available for minimizing the cost of a carbon capture facility, namely, the selection of the solvent molecule. We argue that the selection of the solvent molecule (or a *de novo* molecular design) in conjunction with the design of the process is in effect *the central* element of creating cost-effective capture solutions covering the wide gamut of applications of CO_2 capture from point sources, which will ultimately lead to widespread adoption and a meaningful impact on global CO_2 emissions.

In this context, integrated identification of solvent structures and process conditions is important.[8–10] Computer-aided molecular design (CAMD) methods provide a systematic approach for designing solvent molecules based on process performance criteria.[11–13] The molecular structure adds extra degrees of freedom to integrated design problems, necessitating quantitative relationships that link molecular structures and properties. Group contribution-based approaches are often used to establish such correlations between molecular structure and properties.[14–19]

Integrated material and process design for CO_2 separation has been explored for both absorption-based[17,20,21] and adsorption-based[22–24] processes. The approach that is generally taken involves solving an optimization problem using a representation of the system spanning all relevant length and time scales, including macroscopic energy and material balances for the process, and molecular-level modeling that reflects structure-property relations. The resulting optimization problems are large-scale (involving tens of thousands of equations and decision variables), highly nonlinear, and stiff, meaning that they are theoretically challenging and practically impossible to solve. In addition, the discrete nature of molecular structure adds an integer component to the aforementioned optimization problems, compounding the solution difficulty. To address increased computational complexity, various strategies can be employed, including search-space reduction, using simplified process models, hierarchical decompositions, and the use of data-driven surrogate models.

Another approach to tackle this challenge is through continuous molecular targeting (CoMT).[25–27] CoMT involves considering continuous molecular parameters in physics-based

equations of state, such as perturbed-chain-statistical-associating-fluid theory (PC-SAFT), as degrees of freedom for the integrated design problems. This allows for the identification of optimal hypothetical molecules within the continuous design space (avoiding discrete variables), which is often represented by convex polytopes created from a database of molecules using the corresponding continuous molecular descriptors. Existing molecules can be selected by searching the database for elements whose descriptors are closest (in the norm sense) to the optimized solvent.

The current amine-based technologies for CO_2 capture suffer from high energy demand and environmental concerns due to volatile solvent emissions. As a response, the development of environmentally friendly materials and processes is receiving increased attention. Ionic liquids (ILs) have gained attention for their unique characteristics, including low volatility, high CO_2 affinity, and low toxicity, positioning them as a sustainable solvent.[28–31] In particular, ILs offer a large design space through the combination of cation and anion pairs.

Motivated by the above, we pursue a novel multi-scale modeling and optimization framework of IL-based carbon capture processes. The PC-SAFT model is used to represent IL material properties using continuous and scalable relations.[26,32] Without any additional adjustable parameters, this model can reliably predict important thermodynamic properties, including the density of pure ILs and CO_2 solubility.[33–35] Pseudo-transient continuation is used to impart favorable convergence properties to the optimization problem.[36]

The key contributions of this work are:

- We use a comprehensive process flowsheet model including a detailed rate-based model for CO_2 absorption, which accounts for critical kinetic limitations in mass and heat transfer processes. In particular, viscosity is an important property for mass transfer and we develop a continuous model for predicting viscosity.

- The design space of IL solvents for CoMT is partitioned into cation and anion spaces within the continuous design space. The identification of IL molecules relies on the optimal selection of cation-anion combinations. This approach offers the advantage of expanding the design space with a relatively small number of cation and anion options. Therefore, a large number of (hypothetical) molecules can be efficiently scanned.

Solvent-Based CO_2 Capture From Point Sources

A general configuration of preemptive, point-source carbon capture is illustrated in Figure 1. Preemptive carbon capture refers to the process of capturing carbon dioxide (CO_2) from high-pressure streams, taking advantage of the favorable pressure conditions for efficient capture. This differs from post-combustion carbon capture, which involves capturing CO_2 from flue gases at atmospheric pressure. Preemptive capture aims to remove CO_2 from shifted syngas streams such as those that arise in the operation of power plants using municipal waste[37] or integrated gasification combined cycle (IGCC) configurations,[38,39] as well as from high-pressure CO_2 streams in processes such as steam methane reforming (SMR) for hydrogen production.[40] We utilize preemptive capture of CO_2 to exemplify carbon capture processes, noting that the configuration and operation of post-combustion, atmospheric-pressure systems are fundamentally similar (Figure 1). For preemptive capture, the gas

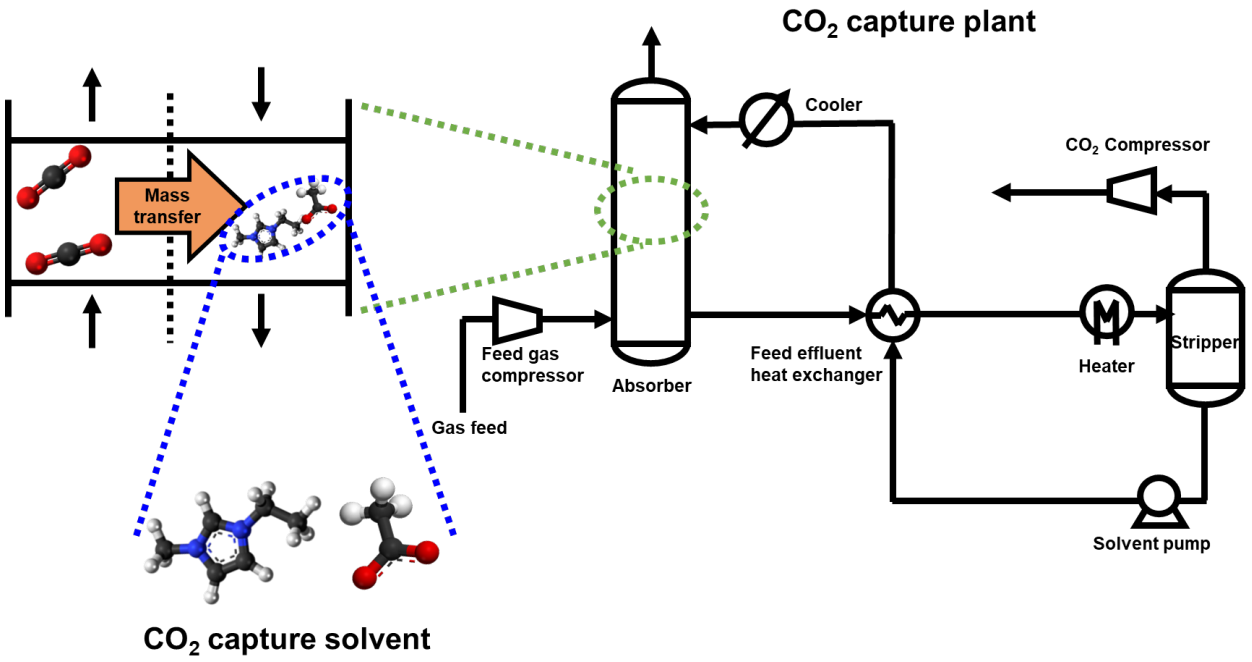

Figure 1: Schematic illustration of the multi-scale nature of the CO_2 capture solvent and process design problem. A general flowsheet configuration for a point-source capture plant is shown. A gas containing CO_2 comes into contact with a solvent in the absorber. The concentration gradient drives mass transfer of CO_2 between the gas and liquid phases, with the solvent leaving the absorber having a high CO_2 concentration. The CO_2 is released in the stripper, producing a CO_2 stream that can be sequestered or further processed. The regenerated solvent is then returned to the absorber. In general, CO_2 absorption is favored by high pressure and low temperature, and CO_2 desorption is favored by high temperature and low pressure. A solvent cooler and feed compressor, and a heater may thus be used to enhance absorption and desorption, respectively. The performance of the CO_2 capture plant (in terms of energy used for heating/cooling, equipment cost) has a complex dependence on the selection of the CO_2 capture solvent molecule, being impacted by its CO_2 absorption enthalpy, heat capacity, viscosity, density, etc.

stream (comprising mostly hydrogen and carbon dioxide) contains 15-60% CO_2, depending on the source application.[41] We focus in particular on ionic liquid (IL) absorbents. Given that the pressure of the gas streams is typically between 2 and 7 MPa,[42] a physical absorbent is preferred for high-pressure capture because solvent regeneration can be achieved by depressurization without having to elevate the temperature for regeneration (resulting in a lower energy requirement). Physically absorbing solvents (such as Selexol and ILs) have been found to provide better economic performance for preemptive capture when compared to the chemically absorbing amine solvents.[43–45] ILs are promising physical solvents for high-pressure CO_2 capture[17,46] due to their superior thermophysical properties including high gas solubility, low volatility, and stability.[31,47]

Multi-Scale CO_2 Capture Process Model

Structure-property relation model using PC-SAFT

At the molecular scale, the model relies on perturbed-chain statistical associating fluid theory (PC-SAFT) extended for electrolyte solutions.[48–50] The PC-SAFT model is used to predict the thermophysical properties of the IL solvent,[51,52] thereby realizing the connection with the macroscopic scale. IL solvents are considered to be completely dissociated into their respective cations and anions. Although many ILs are not completely dissociated,[53] this approach has been shown to adequately represent a variety of IL and IL/CO_2 systems.[35] The *individual* anions and cations are represented in the PC-SAFT model as a function of three *continuous* descriptors, comprising the segment number m, segment diameter σ, and the segment dispersive energy parameter ε/k. A database of 18 cations and 9 anions is considered, resulting in 162 possible ILs. These specific cations and anions are carefully selected from the literature, ensuring the use of all the ILs for which data are available, except for some inappropriate cations/anions (this will be discussed in the next section). The values of the descriptors are fitted using density data for pure ILs.[35] Then, molecular-level properties are predicted as a function of the molecular descriptors of the anion and cation moieties. Accurate property predictions can be obtained without resorting to the use of binary interaction parameters for density, CO_2 solubility, and residual heat capacity.[33–35] Heat capacity is then calculated using an estimate of the ideal gas heat capacity as proposed in Joback and Reid[54]. A continuous-valued expression for the ideal gas heat capacity of ILs as a function of the aforementioned descriptors (PC-SAFT parameters) is obtained as suggested by Stavrou et al.:[26]

$$C_{\mathrm{p}}{}^{\mathrm{ig}} = C_0 + C_1\left(m\frac{\varepsilon}{kT}\right) + C_2\left(m\sigma^3\right) + C_3\left(m\sigma^3\frac{\varepsilon}{kT}\right) \tag{1}$$

where $C_{\mathrm{p}}{}^{\mathrm{ig}}$ is ideal gas heat capacity and C_i are coefficients for each term (Table S5, Figure S2). $C_{\mathrm{p}}{}^{\mathrm{ig}}$ values for other components are estimated based on the summation of group contribution parameters:[54]

$$\begin{aligned} C_{\mathrm{p}}{}^{\mathrm{ig}} = &\left(\sum_k n_k A_{C_p,k} - 37.93\right) + \left(\sum_k B_{C_p,k} + 0.210\right) T \\ &+ \left(\sum_k C_{C_p,k} - 3.91\times10^{-4}\right) T^2 + \left(\sum_k D_{C_p,k} + 2.06\times10^{-7}\right) T^3 \end{aligned} \tag{2}$$

The work of Stavrou et al.[26] is also used to estimate the molar mass for ILs represented by PC-SAFT parameters:

$$M = M_0 + M_1\left(m\frac{\varepsilon}{k}\right) + M_2\left(m\sigma^3\right) + M_3\left(m\sigma^3\frac{\varepsilon}{k}\right) \tag{3}$$

where M is the molar weight and M_i are the coefficients of the correlation (Table S4, Figure S1). The prediction of ideal gas heat capacity and molecular weight is not expected to cause significant errors in the process performance, given the overall accuracy of the results. The

parameter values and accuracy are included in the SI Tables S4 and S5, with visualizations in Figures S1 and S2.

Predicting viscosity is important considering its significant impact on the mass transfer and liquid holdup in the absorption column. Rosenfeld proposed[55,56] a residual entropy scaling theory to predict viscosity for simple fluids. Rosenfeld's original quasi-universal, monovariable relation is limited to ideal spherical monatomic fluids. For general fluids, component-specific parameters or relations are necessary. Recent studies have extended this theory by proposing different structures of entropy scaling terms (e.g.,[57–59]). Motivated by these studies, we propose a combined entropy scaling and Vogel-Fulcher-Tammann (VFT) model that represents viscosity as a function of density, molar weight, temperature, and an entropy scaling term, with the addition of the VFT equation term to account for the temperature dependency of viscosity of ILs:

$$\begin{aligned} \ln \mu_{\mathrm{ES}} =& A_0 + A_1 \ln \rho + A_2 \ln M + A_3 \ln T + A_4(-s) + A_5(-s)^{-1} \\ \ln \mu_{\mathrm{VFT}} =& A_6 \frac{1}{(T - 170K)} \\ \ln \mu =& \ln \mu_{\mathrm{ES}} + \ln \mu_{\mathrm{VFT}} \end{aligned} \tag{4}$$

where $\ln \mu_{\mathrm{ES}}$ is the entropy scaling term, s represents the reduced residual entropy given by $S_{\mathrm{res}}/N_A k$, $\ln \mu_{\mathrm{VFT}}$ is the VFT equation term, and the ideal glass transition temperature is set at a fixed value of 170 K. The regression results and the relevant parameter values are presented in Figure S3 and Table S6.

We note that the proposed viscosity model also captures the reduction in viscosity that occurs when CO_2 is absorbed in the IL. This phenomenon is important to predict since the viscosity of CO_2-rich IL solvents can differ significantly from the viscosity of pure ILs.[60] Previous viscosity prediction models are mostly group-based approaches (i.e., discrete representations) and do not account for reduced viscosity when CO_2 is absorbed.[61–63] The most recent multi-scale optimization study for IL-based carbon capture does not account for this viscosity reduction of IL after CO_2 absorption.[17] Although our regression is based on pure IL properties, our proposed approach accounts for the decreased molar weight, density, and residual entropy for the mixture of CO_2, IL anion, and IL cation, and therefore, the reduced viscosity can be reasonably estimated when CO_2 is absorbed into the IL (Figure S4).

While a single regression model for viscosity can adequately describe various cations, we discover that different anions necessitate different correlation parameters. Using the k-means clustering algorithm,[64,65] we categorize anions into three clusters based on their three-dimensional PC-SAFT parameters as shown in Figure 2 and Table 1. These clusters/groups are then described with specific viscosity correlation models. In addition, the exponent of the model is constrained to be positive to ensure physical realism. Each model is specifically designed for a small design space defined by each group, and we use a wide range of temperature data ranging from 10°C to 100°C, thus overfitting is avoided.

IL molecule design space

Although PC-SAFT parameters for 1,3-dimethyl-imidazolium cation are available (predicted from the linear dependence on molar mass[35]), we exclude this cation from the design

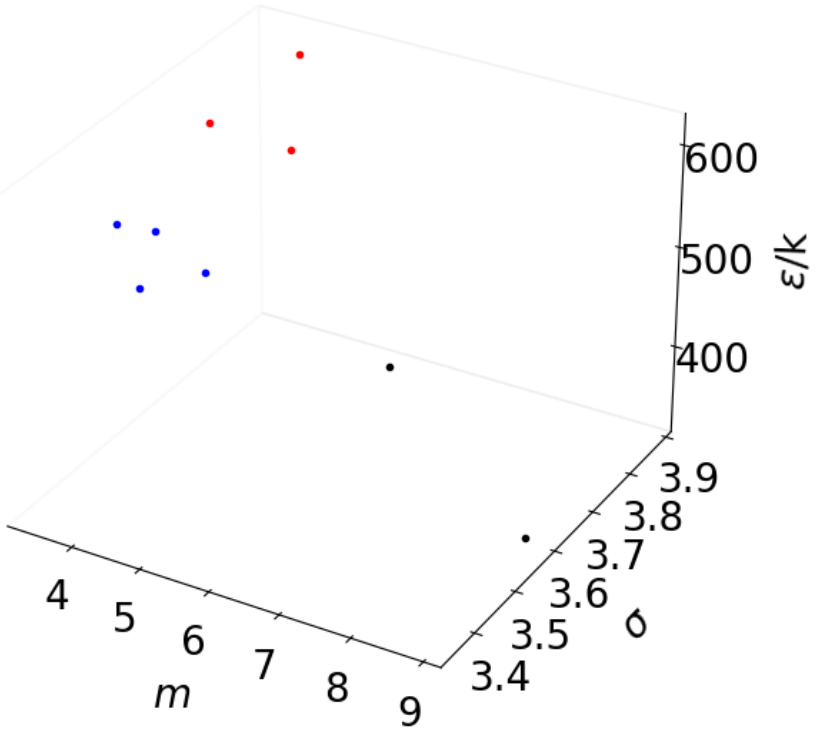

Figure 2: Three anion groups (group 1: $[Tf_2N]^-$, $[eFAP]^-$; group 2: $[TfO]^-$, $[DCA]^-$, $[C_2SO_4]$; group 3: $[BF_4]^-$, $[PF_6]^-$, $[SCN]^-$, $[Ac]^-$). Specific regression models are derived for each cluster/group.

Table 1: Anion cluster groups

Anion		m	σ	ε/k
group 1	$[Tf_2N]^-$	6.01	3.75	375.65
	$[eFAP]^-$	8.84	3.60	318.48
group 2	$[Tfo]^-$	3.74	3.88	509.31
	$[DCA]^-$	3.43	3.73	578.04
	$[C_2SO_4]$	4.14	3.84	623.48
group 3	$[BF_4]^-$	3.82	3.51	496.12
	$[PF_6]^-$	4.28	3.59	492.28
	$[SCN]^-$	4.55	3.36	624.24
	$[Ac]^-$	3.73	3.56	533.11

space because it forms a solid ILs in the temperature range of interest. This is because the symmetry of the cation (due to identical methyl groups) enhances crystallization[66] and the melting point of the dimethyl imidazolium-based IL can be unusually high.[67] Also excluded as unsuitable choices are halide-based[68] ILs that are solid at room temperature and trihexyltetradecylphosphonium-based ILs that are excessively bulky and viscous. Hence, ILs

that exhibit these extreme properties do not contribute in defining our design space.

For most IL cations and anions, the PC-SAFT prediction of CO_2 solubility is acceptable without introducing binary parameters. Given the small number of descriptors and the vast design space, we consider PC-SAFT predictions with a mean absolute percentage error (MAPE) of less than 20 % as acceptable. The solubility predictions for the 33 ILs within our design space are reported by Sun et al.[35] However, some cases (Br^-, $C_1SO_4^-$, and C_nmpy^+-based ILs) require adjustable binary parameters to accurately fit the experimental CO_2 solubility data. For example, the prediction of CO_2 solubility in $[C_6mpy][Tf_2N]$ significantly deviates from the experimental data (70.2% MAPE) when a binary parameter is not used.[35] Therefore, these ILs are excluded from the design space (these cation/anions falls outside of the polytopes defining the design space).

We note that a sensitivity analysis of the process design with respect to key molecular properties (molar volume, heat capacity, and viscosity) was discussed in our previous work,[69] where interested readers can find detailed information.

We show the PC-SAFT parameters used for the design space of IL solvents and the set of linear inequality constraints formed by the convex polytope (which will be described later) of the IL solvent design space in Equations S1 and S2.

CO_2 capture process flowsheet model

At the macroscopic level, material and energy balance equations for the absorber, solvent regenerator (CO_2 stripper), heat exchangers, and compressor are included in the model. Rate-based mass transfer between the gas and liquid phase is considered in the absorber (rather than assuming equilibrium between phases).

We develop a flowsheet model for a preemptive carbon capture process using our previous work[69] with minor modifications.

- The overall mass transfer coefficient, K_{g,CO_2} can be represented as:

$$\frac{1}{K_{g,CO_2}} = \frac{1}{k_{g,CO_2}} + \frac{1}{k_{l,CO_2}} \tag{5}$$

  where k_{g,CO_2} and k_{l,CO_2} are the gas-phase and liquid-phase mass transfer coefficients for CO_2 gas. Since we consider physical absorption only in this work, a correlation factor that quantifies enhanced mass transfer due to chemical absorption of CO_2 is not included.

  The viscosity of ILs can be high compared to aqueous solvents (e.g., viscosity for $[C_6mim][Tf_2N]$ is 55 cP at 30 ^oC). Song et al.[70] developed a general mass transfer correlation for viscous fluids using aqueous glycerol (up to ∼70 cP):

$$k_{g,CO_2} = \frac{0.28}{RT} U_V^{0.62} \left(\frac{\mu_V}{\rho_V}\right)^{-0.12} \left(D_{CO_2}^V\right)^{0.5} a_p^{0.38} \tag{6}$$

$$k_{l,CO_2} = 0.12\, U_L^{0.565} \left(\frac{\mu_L}{\rho_L}\right)^{-0.4} \left(D_{CO_2}^L\right)^{0.5} g^{1/6} a_p^{-0.0065} \left(\frac{L_{column}}{1.8}\right)^{-0.54} \tag{7}$$

where μ is viscosity, ρ is density, U is superficial velocity, $D_{\mathrm{CO_2}}$ is the diffusion coefficient of CO_2, and g is the acceleration of gravity. The subscript or superscript V and L represent vapor and liquid phase properties, respectively. a_{p} is the specific surface area of packing, L_{column} is the packing height.

- The energy transfer rate (between liquid and vapor phase in the absorption column), N_{H} is calculated as the sum of the enthalpy change by bulk CO_2 flow and convective heat transfer:

$$N_{\mathrm{H}} = N^{\mathrm{L}}_{\mathrm{CO_2}} \Delta H + h a_{\mathrm{e}} \left(T^{\mathrm{V}} - T^{\mathrm{L}}\right) \tag{8}$$

where $N^{\mathrm{L}}_{\mathrm{CO_2}}$ refers to molar transfer rate of CO_2 gas, and ΔH denotes the molar enthalpy change due to mixing with CO_2 flow (the change of enthalpy with respect to increase of CO_2 concentration at given temperature T^{L} is simultaneously calculated by the PC-SAFT model). The $h a_{\mathrm{e}} \left(T^{\mathrm{V}} - T^{\mathrm{L}}\right)$ term describes the convective transfer rate. The convective heat transfer coefficient, h is estimated using the Chilton-Colburn analogy. This analogy relates the heat transfer coefficient to the mass transfer coefficient:[71]

$$h = K_{\mathrm{g,CO_2}} \left(\frac{C^{\mathrm{V}} C^{\mathrm{V}}_p (\kappa^{\mathrm{V}})^2}{(D^{\mathrm{V}}_{\mathrm{CO_2}})^2} \right)^{1/3} \tag{9}$$

where C^{V} is the molar density (reciprocal of molar volume), and C^{V}_p and κ^{V} are the heat capacity and thermal conductivity of the vapor phase. $D^{\mathrm{V}}_{\mathrm{CO_2}}$ represents the diffusion coefficient of CO_2 in the vapor phase.

The column effective packing area, a_{e} is:[70]

$$a_{\mathrm{e}} = a_{\mathrm{p}} \left[1.16\, \eta_{\mathrm{p}} \left(\mathrm{We_L Fr_L^{-0.5}} \right)^{0.138} \right] \tag{10}$$

where η_{p} is a packing correction factor, and $\mathrm{We_L}$ and $\mathrm{Fr_L}$ refer to the Weber and Froude numbers for the liquid phase.

- IL solvent regeneration is performed using multiple flash units at different pressures. As shown in Figure S5, We use two flash units (medium-pressure flash and low-pressure flash units) based on the work by Zhai and Rubin.[46] Flash units are assumed to be at equilibrium and the corresponding vapor-liquid equilibrium for CO_2-IL system is estimated by the PC-SAFT model.

To address convergence difficulties typically encountered in solving high-dimensional, nonlinear optimization problems (specifically, IL-based carbon capture processes which incorporate detailed thermodynamic and rate-based models as described before), we use the pseudo-transient modeling approach proposed by Pattison et el.[36] This method involves reformulating the original algebraic equation system as a differential algebraic equation system with the dynamics governed by a set of pseudo-time constants. A comprehensive description of this modeling and reformulation procedure can be found in our previous work.[69]

Optimization problem formulation for multi-scale design

The simultaneous design of the process and IL solvent is formulated as an optimization problem of the form:

$$\begin{aligned} \min_{x,y,z} \quad & f(x,\theta,z) \\ \text{s.t.} \quad & h_{\mathrm{p}}(x,\theta,z) = 0 \\ & \theta = h_{\mathrm{m}}(x,y) \\ & g_{\mathrm{p}}(x,\theta,z) \leq 0 \\ & g_{\mathrm{m}}(y) \leq 0 \\ & x_{\mathrm{lb}} \leq x \leq x_{\mathrm{ub}} \\ & y_{\mathrm{lb}} \leq y \leq y_{\mathrm{ub}} \\ & z_{\mathrm{lb}} \leq z \leq z_{\mathrm{ub}} \end{aligned} \tag{11}$$

where f is the annualized cost for the CO_2 capture process. We consider capital costs (absorber, flash tanks, pump, heat exchanger, steam heater, cooler, and compressors) and operating costs (electricity, heating, and cooling). The variable vector x represents the process operating variables (e.g., process temperatures, pressures, and flowrates), y represents molecular descriptors (PC-SAFT parameters), and z represents the process design variables (e.g., height and diameter of the absorber). The equation vector h_p represents the macroscopic model equations (e.g., mass and energy balances, rate-based mass transfer model), θ represents the molecular properties, and h_{m} are equations representing the structure-property relations based on the PC-SAFT model as described above. g_{p} and g_{m} are process and molecular constraints, respectively. The subscripts "lb" and "ub" indicate lower and upper bounds on the variables, respectively. The molecular constraints, g_{m}, y_{lb}, and y_{ub} are different for each viscosity-group subproblem. Process-level decision variables, constraints, and molecular-level constraints are presented in Table S1, and Equations S1 and S2.

We present detailed cost correlation models used in this work in the Supporting Information. We use a value of 5.0 for the scaling factor (a factor that converts purchased equipment cost to total capital cost) and a value of 0.2 for the annualizing factor (a factor that annualizes capital cost and addresses return on investment, tax, depreciation, and maintenance).[72]

There are four optional units (feed compressor, cooler, heater, and heat exchanger) in the flowsheet model (Figure S5). We note that the cost for each optional unit is active only if the corresponding unit is necessary (i.e., both capital and operating costs related to the equipment are zero if it is not included). This is because the purchased equipment cost for each unit is zero when the cost sizing factor (heat exchange area for cooler, heater, heat exchanger, and compressor work for feed gas compressor) is zero. For the heat exchanger model, the approach temperature for a heat exchanger is not constrained to a specified minimum approach temperature as in[69] to ensure the case of the absence of a heat exchanger. Although a minimum approach temperature is not specified, there is a trade-off between high heat integration, i.e. a low approach temperature, and expensive heat exchanger cost (due to high heat exchanger area), and a (physically) reasonable value is obtained.

The optimization problem formulated above is constrained at the macroscopic level by

g_p, a set of constraints that includes overall CO_2 capture level, temperature limits for cooling and heating, etc.

In order to account for the different viscosity correlations for the three different sets of anions, we consider three subproblems, where each subproblem uses different viscosity correlations and constraints for the anion descriptors. Then, we optimize each submodel and determine the minimum objective value and the corresponding decision variables. This approach effectively addresses the diverse viscosity behaviors exhibited by different sets of anions.

Molecular level constraints g_m are defined under two different circumstances:

- *Solvent selection*: Here, g_m are defined to ensure the physical existence of the optimal molecular structure. Specifically, the search space of the PC-SAFT descriptors is confined to the convex polytope formed by descriptors of the known cation and anion moieties available in the database (Figure S6).

- *Solvent discovery*: Here, the g_m constraints are relaxed by expanding the convex hull formed by descriptors of the known cations in each coordinate direction by an adjustable weight $\alpha > 1$. For anions, the molecular descriptors are confined to a range defined by their respective minimum and maximum values for the entities in each cluster. That is, the constraints on g_m are replaced by a box constraint of the type $y_{\text{lb}} \leq y \leq y_{\text{ub}}$ (Figure S7).

The flowsheet model for each subproblem has ∼35,000 equations and is implemented in gPROMS ProcessBuilder. These problems are solved within the range of 2 to 4 hours of CPU time (for each subproblem in both solvent selection and discovery) on a 64 bit Windows 10 PC with an Intel Core i7, 3.20 GHz processor and 16.0 GB RAM.

Results and Discussion

In this work, we consider various feed gas conditions, which have different CO_2 compositions and pressures (15 mol%, 22.5 bar; 22 mol mol%, 22.5 bar; 37 mol%, 29.6 bar; 60 mol%, 29.6 bar) representing a broad range of possible gas conditions from power generation or SMR plants,[40,41,46] as shown in Table 2. H_2 and CH_4 are considered inert, as their solubilities in ILs are remarkably lower than that of CO_2[73,74] Additionally, different levels of carbon capture rates (90 %, 95 %, and 99 %) are taken into account.

Table 2: Feed gas conditions

CO_2 (mol%)	15	22	37	60
H_2/CH_4 (mol%)	85	78	63	40
Flowrate (kmol/h)	13,950			
Pressure (bar)	22.5	22.5	29.6	29.6

The optimal IL selection and corresponding capture costs are presented in Figure 3. For comparison, other studies have estimated the pre-combustion carbon capture cost for IGCC

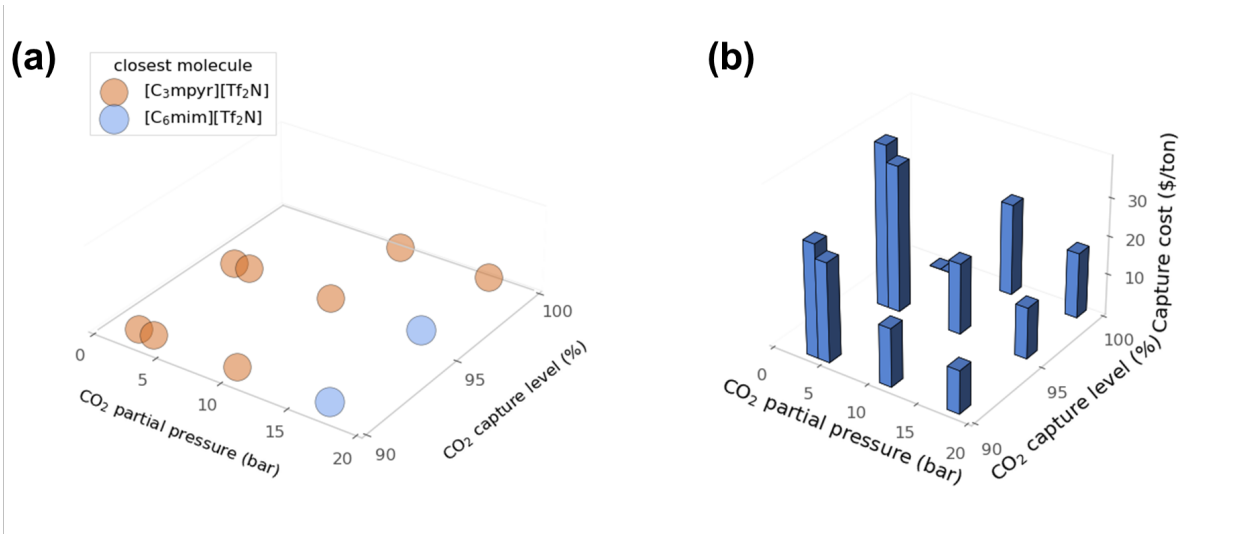

Figure 3: (a) Optimal IL selection and (b) process cost as a function of feed CO_2 partial pressure and target capture level.

power plants using amine-based solvent to be Euro 25.3/tonne[44] and GBP 9.1/tonne.[75] The results in Figure 3 are competitive with these values, within the uncertainty of the capital and operating cost estimates. The results are highly dependent on the specific point sources and carbon capture levels. For cases with higher capture rates and lower partial pressure in the gas feed, the capture cost is found to be higher primarily due to higher energy and larger process unit requirements. In general, the absorption process requires higher pressure and lower temperatures and the regeneration process requires higher temperatures to achieve the desired CO_2 capture level. Consequently, larger absorber, heat exchanger, and regeneration units are needed to accommodate the higher solvent requirements. In such cases, smaller molecules ([C_3mpyr][Tf_2N]) are preferred because of their smaller specific volumes, which help to avoid larger equipment sizes and the higher cost of pumping. Also, it is because of their lower heat capacities, which will prevent excessive cooling/heating costs during the process.

In contrast, for cases with higher partial pressure of CO_2 and lower CO_2 capture levels, relatively smaller solvent amounts and less energy are required. Therefore, molecular specific volume and heat capacity are less important than in the former cases, and relatively larger molecules ([C_6mim][Tf_2N]) are preferred to achieve a higher CO_2 cyclic capacity. However, excessively large molecules, which have higher viscosities, are avoided.

There are no feasible solutions found for high capture levels and low-pressure cases under the operating constraints (maximum allowable compression pressure is 60 bar and flash temperature is 100 °C).

It has been reported that [C_6mim][Tf_2N] is an effective absorbent for CO_2 capture because of its stability, low viscosity, and selective (high) CO_2 solubility.[76] A [C_6mim][Tf_2N]-based carbon capture system was compared to a well-established technology (Selexol-based).[46] The results showed a 3.1 % reduction in overall capture costs for the [C_6mim][Tf_2N]-based system compared to the Selexol-based system. Therefore, we use the [C_6mim][Tf_2N]-based system as the baseline/benchmark in this paper.

Although [C_6mim][Tf_2N] is also identified as an effective solvent for high-pressure capture cases in our study, we find that another solvent ([C_3mpyr][Tf_2N]) performs better in other applications. Therefore, we compare our findings with the case of this benchmark IL solvent ([C_6mim][Tf_2N]) using a subset (in terms of the CO_2 partial pressure and capture rate) of the scenarios described earlier ((a) 22 mol% CO_2 content, 22.5 bar feed pressure, 90 % capture level, (b) 37 mol% CO_2 content, 29.6 bar feed pressure, 90 % capture level, (c) 22 mol% CO_2 content, 22.5 bar feed pressure, 99 % capture level). These particular scenarios are chosen because their solvent decisions differ from the benchmark IL ([C_6mim][Tf_2N]).

Both processes (i.e., using the baseline solvent and allowing for new solvent selection) are optimized using the same cost correlation models with fixed material choices. Figure S8 and S9 show capital and operating costs of the optimal and benchmark systems. For all cases, both capital and operating costs are smaller for the system using the optimized IL. This can be attributed to the smaller size of the equipment and lower heat duties required for cooling and heating (note that heat duties related to cooling and heating are non-zero only for case (c)). This is because a larger size of equipment is necessary for the benchmark IL process due to the higher molar volume (Table 3). Note that the capital cost is primarily defined by the equipment sizes, which directly depend on the solvent volume. Similarly, operating and utility costs including heating and cooling are much higher for the benchmark IL process because the heat capacity of the benchmark IL is higher (Table 3). Overall, the CO_2 capture process using the optimal IL (([C_3mpyr][Tf_2N])) can achieve up to 13.4% cost savings (case (a): 9.4%, case (b): 6.9%, case (c): 13.4%) compared to the benchmark IL-based carbon capture process. These results show that improved material selection and process design can be reached through the multi-scale design, therefore securing large economic savings in overall process costs.

Table 3: Comparison of properties between the benchmark IL ([C_6mim][Tf_2N]) and the optimal IL ([C_3mpyr][Tf_2N])

Property*	[C_6mim][Tf_2N]	[C_3mpyr][Tf_2N]
molar volume (cm^3/mol)	327.8	193.0
heat capacity (J/K mol)	671.3	339.5

*The properties are predicted by the PC-SAFT model at 30 ^{o}C and 1 bar.

Figure 4 shows a comparison of CO_2 solubility between the benchmark IL ([C_6mim][Tf_2N]) and the optimal IL ([C_3mpyr][Tf_2N]). Although the apparent CO_2 molar capacity is higher for the benchmark IL, this choice of solvent molecule does not lead to savings in process costs because the process-level considerations are neglected. The multi-scale design problem evaluates the properties of the IL solvent, specifically identifying a molecule with relatively high volumetric CO_2 capacity to avoid higher liquid volume (which causes larger equipment size and expensive pumping). Similarly, a molecule with higher heat capacity is avoided to keep heating/cooling costs low (in particular, for case (c)). To this end, an IL solvent with balanced properties (relatively high volumetric CO_2 capacity and low heat capacity) is selected considering the impact on process-level costs.

Finally, we optimize the carbon capture process by expanding the molecular design space.

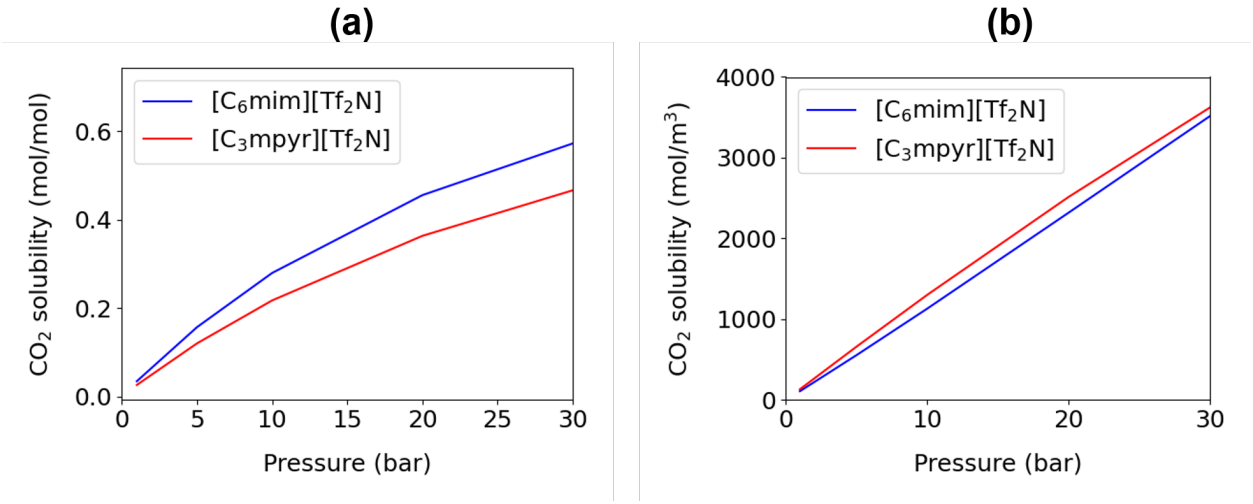

Figure 4: Comparison of (a) molar solubility and (b) volumetric solubility between the benchmark IL ([C_6mim][Tf_2N]) and the optimal IL ([C_3mpyr][Tf_2N]). CO_2 solubility is predicted by PC-SAFT model.

We ambitiously assume that it would be possible to increase the cation design space (represented by the three PC-SAFT parameters) by 50% in each parameter direction. Likewise, we assume the anion convex polytope could be expanded to a box space represented by the minimum and maximum bounds of the three PC-SAFT parameters (Figure S7). Given the absence of a definitive approach for predicting what is feasible, experimental efforts to establish a reasonable expansion range are essential. The aim of this expansion is to provide insights for molecule synthesis and the identification of superior molecules. This expanded design space led to the suggestion of a new solvent, as presented in Supporting Information (Figure S10, Table S2). To evaluate this potentially new IL solvent, we use a representative example with a carbon point source containing 37 mol % CO_2, a feed pressure of 29.6 bar, and a process constraint of 90 % capture level.

The molecular size (the effective molecular size can be estimated by the m and σ values of the molecule) plays a critical role in determining the solubility of CO_2 in ILs. For instance, a larger molecule may have stronger van der Waals interactions with CO_2 molecules, contributing to the enthalpic driving force for solubility. The energy parameter (ε) can impact the balance of interactions between cation-anion and anion-CO_2 entities. These molecular parameters affect other physical properties, such as density, heat capacity, and viscosity. By expanding the design space, we can identify more balanced IL molecules and ultimately an optimal IL molecule with a higher cyclic capacity without a significant increase in heat capacity and specific volume (Table 4).

The synthesis of molecules based on (the optimal) molecular descriptors, is still an open question and an important direction for future research. Experimental validation would be necessary to determine if the optimized molecule can be realized and exhibits the desired properties in practice. In the expanded PC-SAFT parameter design space, the new optimal IL lies on a bound (Table S2 and Figure S10); however, the thermophysical properties of the new optimal IL (Table 4) represent a balance between higher values of heat capacity and

molar volume (both disadvantageous) and higher CO_2 solubility (advantageous and enabling higher cyclic capacity), with all of these properties well within reasonable bounds for ILs.

Table 4: Comparison of properties of optimal ILs using original design space and expanded design space

Property	Original design space	Expanded design space
molar volume (cm^3/mol)	193.0	242.5
heat capacity (J/K mol)	339.5	352.7
Cyclic capacity (mol/mol)	0.419	0.579

*The properties are predicted by the PC-SAFT model at 30 ^{o}C and 1 bar.

Conclusions

A multi-scale optimization framework is developed for the simultaneous optimization of process design/conditions and material selection for preemptive, high-pressure CO_2 capture processes using ionic liquids (ILs). The approach introduced in this work uses a pseudo-transient modeling technique, which makes it possible to solve difficult numerical problems using general-purpose commercial solvers. Moreover, key molecular properties including CO_2 solubility, density, heat capacity, and viscosity are represented continuously using the PC-SAFT model. The design space for ILs is restricted within the convex polytope constructed by PC-SAFT parameters. For the process level, detailed cost models for the process equipment and a rigorous rate-based absorption model are employed. We identify the optimal IL solvent and the corresponding process design simultaneously. The material design captures the inherent economic trade-off (e.g., between CO_2 absorption capacity and equipment sizes/energy requirements) of the process. The multi-scale approach achieves significant cost savings compared to the optimal process design using a benchmark IL solvent. Increasing the design space of molecules further improves the process efficiency by identifying unknown ionic liquids. Synthesizing such a molecule would indeed pose a significant challenge, necessitating experimental efforts to further explore this space. Furthermore, experimental validation of properties such as absorption and desorption kinetics is essential for improving the accuracy of the multi-scale design. The multi-scale framework introduced is general and versatile so it can be used for many applications beyond the case study of high-pressure CO_2 capture using ionic liquids. There are ongoing efforts to describe key thermodynamic properties and establish correlations with molecular structure, as this is a fundamental requirement for the extension of this framework for low-pressure CO_2 capture (using chemical absorption solvents).

Acknowledgments

The authors acknowledge the financial support provided by ExxonMobil through the Fueling a Sustainable Energy Transition (FSET) program of the University of Texas at Austin Energy Institute. K.S. was partially supported by the Phillips 66 Fellowship and

the Graduate School Continuing Fellowship at the University of Texas. Partial financial support from the National Science Foundation under the ECO CBET award 2133543 is also acknowledged.

References

(1) Cresko, J. et al. Industrial Decarbonization Roadmap. US Department of Energy DOE/EE-2635, 2022.

(2) Rochelle, G.; Chen, E.; Freeman, S.; Van Wagener, D.; Xu, Q.; Voice, A. Aqueous piperazine as the new standard for CO_2 capture technology. *Chemical Engineering Journal* **2011**, *171*, 725–733.

(3) Tsay, C.; Pattison, R. C.; Zhang, Y.; Rochelle, G. T.; Baldea, M. Rate-based Modeling and Economic Optimization of Next-generation Amine-based Carbon Capture Plants. *Applied Energy* **2019**, *252*, 113379.

(4) Zhang, X.; Zhang, X.; Dong, H.; Zhao, Z.; Zhang, S.; Huang, Y. Carbon capture with ionic liquids: overview and progress. *Energy and Environmental Science* **2012**, *5*, 6668–6681.

(5) Shama, V. M.; Swami, A. R.; Aniruddha, R.; Sreedhar, I.; Reddy, B. M. Process and engineering aspects of carbon capture by ionic liquids. *Journal of CO_2 Utilization* **2021**, *48*, 101507.

(6) Zheng, R. F.; Barpaga, D.; Mathias, P. M.; Malhotra, D.; Koech, P. K.; Jiang, Y.; Bhakta, M.; Lail, M.; V. Rayer, A.; Whyatt, G. A.; Freeman, C. J.; Zwoster, A. J.; Weitz, K. K.; Heldebrant, D. J. A single-component water-lean post-combustion CO_2 capture solvent with exceptionally low operational heat and total costs of capture – comprehensive experimental and theoretical evaluation. *Energy & Environmental Science* **2020**, *13*, 4106–4113.

(7) Heldebrant, D. J.; Kothandaraman, J.; Dowell, N. M.; Brickett, L. Next steps for solvent-based CO_2 capture; integration of capture, conversion, and mineralisation. *Chemical Science* **2022**, *13*, 6445–6456.

(8) Eden, M.; Jørgensen, S.; Gani, R.; El-Halwagi, M. A novel framework for simultaneous separation process and product design. *Chemical Engineering and Processing: Process Intensification* **2004**, *43*, 595–608.

(9) Gopinath, S.; Jackson, G.; Galindo, A.; Adjiman, C. Outer approximation algorithm with physical domain reduction for computer-aided molecular and separation process design. *AIChE Journal* **2016**, *62*, 3484–3504.

(10) Adjiman, C. S.; Sahinidis, N. V.; Vlachos, D. G.; Bakshi, B.; Maravelias, C. T.; Georgakis, C. Process Systems Engineering Perspective on the Design of Materials and Molecules. *Industrial & Engineering Chemistry Research* **2021**, *60*, 5194–5206.

(11) Gani, R. Computer-Aided Methods and Tools for Chemical Product Design. *Chemical Engineering Research and Design* **2004**, *82*, 1494–1504, Product Design and Engineering.

(12) Papadopoulos, A.; Linke, P. A Unified Framework for Integrated Process and Molecular Design. *Chemical Engineering Research and Design* **2005**, *83*, 674–678.

(13) Adjiman, C. S.; Galindo, A.; Jackson, G. In *Proceedings of the 8th International Conference on Foundations of Computer-Aided Process Design*; Eden, M. R., Siirola, J. D., Towler, G. P., Eds.; Computer Aided Chemical Engineering; Elsevier, 2014; Vol. 34; pp 55–64.

(14) Papadopoulos, A. I.; Stijepovic, M.; Linke, P. On the systematic design and selection of optimal working fluids for Organic Rankine Cycles. *Applied Thermal Engineering* **2010**, *30*, 760–769.

(15) Cignitti, S.; Mansouri, S. S.; Woodley, J. M.; Abildskov, J. Systematic Optimization-Based Integrated Chemical Product–Process Design Framework. *Industrial & Engineering Chemistry Research* **2018**, *57*, 677–688.

(16) Lee, Y. S.; Graham, E. J.; Galindo, A.; Jackson, G.; Adjiman, C. S. A comparative study of multi-objective optimization methodologies for molecular and process design. *Computers & Chemical Engineering* **2020**, *136*, 106802.

(17) Zhang, X.; Ding, X.; Song, Z.; Zhou, T.; Sundmacher, K. Integrated ionic liquid and rate-based absorption process design for gas separation: Global optimization using hybrid models. *AIChE Journal* **2021**, *67*, e17340.

(18) Gertig, C.; Kröger, L.; Fleitmann, L.; Scheffczyk, J.; Bardow, A.; Leonhard, K. Rx-COSMO-CAMD: Computer-Aided Molecular Design of Reaction Solvents Based on Predictive Kinetics from Quantum Chemistry. *Industrial & Engineering Chemistry Research* **2019**, *58*, 22835–22846.

(19) Austin, N. D.; Sahinidis, N. V.; Konstantinov, I. A.; Trahan, D. W. COSMO-based computer-aided molecular/mixture design: A focus on reaction solvents. *AIChE Journal* **2018**, *64*, 104–122.

(20) Oyarzún, B.; Bardow, A.; Gross, J. Integration of process and solvent design towards a novel generation of CO_2 absorption capture systems. *Energy Procedia* **2011**, *4*, 282–290.

(21) Ahmad, M. Z.; Hashim, H.; Mustaffa, A. A.; Maarof, H.; Yunus, N. A. Design of energy efficient reactive solvents for post combustion CO_2 capture using computer aided approach. *Journal of Cleaner Production* **2018**, *176*, 704–715.

(22) Hasan, M. F.; First, E. L.; Boukouvala, F.; Floudas, C. A. A multi-scale framework for CO_2 capture, utilization, and sequestration: CCUS and CCU. *Computers & Chemical Engineering* **2015**, *81*, 2–21.

(23) Liu, T.; First, E. L.; Hasan, M. F.; Floudas, C. A. A multi-scale approach for the discovery of zeolites for hydrogen sulfide removal. *Computers & Chemical Engineering* **2016**, *91*, 206–218.

(24) Hasan, M. F.; First, E. L.; Floudas, C. A. Discovery of novel zeolites and multi-zeolite processes for p-xylene separation using simulated moving bed (SMB) chromatography. *Chemical Engineering Science* **2017**, *159*, 3–17.

(25) Bardow, A.; Steur, K.; Gross, J. Continuous-Molecular Targeting for Integrated Solvent and Process Design. *Industrial & Engineering Chemistry Research* **2010**, *49*, 2834–2840.

(26) Stavrou, M.; Lampe, M.; Bardow, A.; Gross, J. Continuous Molecular Targeting–Computer-Aided Molecular Design (CoMT–CAMD) for Simultaneous Process and Solvent Design for CO_2 Capture. *Industrial & Engineering Chemistry Research* **2014**, *53*, 18029–18041.

(27) Schilling, J.; Lampe, M.; Gross, J.; Bardow, A. 1-stage CoMT-CAMD: An approach for integrated design of ORC process and working fluid using PC-SAFT. *Chemical Engineering Science* **2017**, *159*, 217–230.

(28) Faisal Elmobarak, W.; Almomani, F.; Tawalbeh, M.; Al-Othman, A.; Martis, R.; Rasool, K. Current status of CO2 capture with ionic liquids: Development and progress. *Fuel* **2023**, *344*, 128102.

(29) Wu, Y.; Xu, J.; Mumford, K.; Stevens, G. W.; Fei, W.; Wang, Y. Recent advances in carbon dioxide capture and utilization with amines and ionic liquids. *Green Chemical Engineering* **2020**, *1*, 16–32.

(30) Mota-Martinez, M. T.; Brandl, P.; Hallett, J. P.; Mac Dowell, N. Challenges and Opportunities for the Utilisation of Ionic Liquids as Solvents for CO_2 Capture. *Molecular Systems Design and Engineering* **2018**, *3*, 560–571.

(31) Aghaie, M.; Rezaei, N.; Zendehboudi, S. A Systematic Review on CO_2 Capture with Ionic Liquids: Current Status and Future Prospects. *Renewable and Sustainable Energy Reviews* **2018**, *96*, 502–525.

(32) Lampe, M.; Stavrou, M.; Schilling, J.; Sauer, E.; Gross, J.; Bardow, A. Computer-aided molecular design in the continuous-molecular targeting framework using group-contribution PC-SAFT. *Computers & Chemical Engineering* **2015**, *81*, 278–287.

(33) Ji, X.; Held, C.; Sadowski, G. Modeling imidazolium-based ionic liquids with ePC-SAFT. *Fluid Phase Equilibria* **2012**, *335*, 64–73.

(34) Ji, X.; Held, C. Modeling the density of ionic liquids with ePC-SAFT. *Fluid Phase Equilibria* **2016**, *410*, 9–22.

(35) Sun, Y.; Schemann, A.; Held, C.; Lu, X.; Shen, G.; Ji, X. Modeling Thermodynamic Derivative Properties and Gas Solubility of Ionic Liquids with ePC-SAFT. *Industrial & Engineering Chemistry Research* **2019**, *58*, 8401–8417.

(36) Pattison, R. C.; Baldea, M. Equation-oriented Flowsheet Simulation and Optimization Using Pseudo-transient Models. *AIChE Journal* **2014**, *60*, 4104–4123.

(37) Yang, Y.; Liew, R. K.; Tamothran, A. M.; Foong, S. Y.; Yek, P. N. Y.; Chia, P. W.; Tran, T. V.; Peng, W.; Lam, S. S. Gasification of refuse-derived fuel from municipal solid waste for energy production: a review. *Environmental Chemistry Letters* **2021**, *19*, 2127—2140.

(38) Olabi, A.; Obaideen, K.; Elsaid, K.; Wilberforce, T.; Sayed, E. T.; Maghrabie, H. M.; Abdelkareem, M. A. Assessment of the pre-combustion carbon capture contribution into sustainable development goals SDGs using novel indicators. *Renewable and Sustainable Energy Reviews* **2022**, *153*, 111710.

(39) Jansen, D.; Gazzani, M.; Manzolini, G.; van Dijk, E.; Carbo, M. Pre-combustion CO_2 capture. *International Journal of Greenhouse Gas Control* **2015**, *40*, 167–187.

(40) Katebah, M.; Al-Rawashdeh, M.; Linke, P. Analysis of hydrogen production costs in Steam-Methane Reforming considering integration with electrolysis and CO_2 capture. *Cleaner Engineering and Technology* **2022**, *10*, 100552.

(41) Godin, J.; Liu, W.; Ren, S.; Xu, C. C. Advances in recovery and utilization of carbon dioxide: A brief review. *Journal of Environmental Chemical Engineering* **2021**, *9*, 105644.

(42) Theo, W. L.; Lim, J. S.; Hashim, H.; Mustaffa, A. A.; Ho, W. S. Review of pre-combustion capture and ionic liquid in carbon capture and storage. *Applied Energy* **2016**, *183*, 1633–1663.

(43) Padurean, A.; Cormos, C.-C.; Agachi, P.-S. Pre-combustion carbon dioxide capture by gas–liquid absorption for Integrated Gasification Combined Cycle power plants. *International Journal of Greenhouse Gas Control* **2012**, *7*, 1–11.

(44) Cormos, A.-M.; Cormos, C.-C. Techno-economic assessment of combined hydrogen & power co-generation with carbon capture: The case of coal gasification. *Applied Thermal Engineering* **2019**, *147*, 29–39.

(45) Smith, K. H.; Ashkanani, H. E.; Morsi, B. I.; Siefert, N. S. Physical solvents and techno-economic analysis for pre-combustion CO_2 capture: A review. *International Journal of Greenhouse Gas Control* **2022**, *118*, 103694.

(46) Zhai, H.; Rubin, E. S. Systems Analysis of Physical Absorption of CO_2 in Ionic Liquids for Pre-Combustion Carbon Capture. *Environmental Science & Technology* **2018**, *52*, 4996–5004.

(47) Ramdin, M.; Loos, T.; Vlugt, T. State-of-the-Art of CO_2 Capture with Ionic Liquids. *Industrial & Engineering Chemistry Research* **2012**, *51*, 8149–8177.

(48) Cameretti, L. F.; Sadowski, G.; Mollerup, J. M. Modeling of Aqueous Electrolyte Solutions with Perturbed-Chain Statistical Associated Fluid Theory. *Industrial & Engineering Chemistry Research* **2005**, *44*, 3355–3362.

(49) Held, C.; Cameretti, L. F.; Sadowski, G. Modeling aqueous electrolyte solutions: Part 1. Fully dissociated electrolytes. *Fluid Phase Equilibria* **2008**, *270*, 87–96.

(50) Held, C.; Reschke, T.; Mohammad, S.; Luza, A.; Sadowski, G. ePC-SAFT revised. *Chemical Engineering Research and Design* **2014**, *92*, 2884–2897.

(51) Gross, J.; Sadowski, G. Perturbed-Chain SAFT: An Equation of State Based on a Perturbation Theory for Chain Molecules. *Industrial & Engineering Chemistry Research* **2001**, *40*, 1244–1260.

(52) Gross, J.; Sadowski, G. Application of the Perturbed-Chain SAFT Equation of State to Associating Systems. *Industrial & Engineering Chemistry Research* **2002**, *41*, 5510–5515.

(53) Nordness, O.; Brennecke, J. F. Ion Dissociation in Ionic Liquids and Ionic Liquid Solutions. *Chemical Reviews* **2020**, *120*, 12873–12902.

(54) Joback, K.; Reid, R. Estimation of pure-component properties from group-contributions. *Chemical Engineering Communications* **1987**, *57*, 233–243.

(55) Rosenfeld, Y. Relation between the transport coefficients and the internal entropy of simple systems. *Physical Review A* **1977**, *15*, 2545–2549.

(56) Rosenfeld, Y. A quasi-universal scaling law for atomic transport in simple fluids. *Journal of Physics: Condensed Matter* **1999**, *11*, 5415—-5427.

(57) Lötgering-Lin, O.; Gross, J. Group Contribution Method for Viscosities Based on Entropy Scaling Using the Perturbed-Chain Polar Statistical Associating Fluid Theory. *Industrial & Engineering Chemistry Research* **2015**, *54*, 7942–7952.

(58) Lötgering-Lin, O.; Fischer, M.; Hopp, M.; Gross, J. Pure Substance and Mixture Viscosities Based on Entropy Scaling and an Analytic Equation of State. *Industrial & Engineering Chemistry Research* **2018**, *57*, 4095–4114.

(59) Li, X.; Kang, K.; Gu, Y.; Wang, X. Viscosity prediction of pure refrigerants applying the residual entropy scaling theory coupled with a "Generalized Chart" parametrization method for the Statistical Associating Fluid Theory. *Journal of Molecular Liquids* **2022**, *367*, 120479.

(60) Liu, Z.; Wu, W.; Han, B.; Dong, Z.; Zhao, G.; Wang, J.; Jiang, T.; Yang, G. Study on the Phase Behaviors, Viscosities, and Thermodynamic Properties of CO_2/[C_4mim][PF_6]/Methanol System at Elevated Pressures. *Chemistry — A European Journal* **2003**, *9*, 3897–903.

(61) Yan, F.; He, W.; Jia, Q.; Wang, Q.; Xia, S.; Ma, P. Prediction of ionic liquids viscosity at variable temperatures and pressures. *Chemical Engineering Science* **2018**, *184*, 134–140.

(62) Paduszyński, K.; Domańska, U. Viscosity of Ionic Liquids: An Extensive Database and a New Group Contribution Model Based on a Feed-Forward Artificial Neural Network. *Journal of Chemical Information and Modeling* **2014**, *54*, 1311–1324.

(63) Koi, Z. K.; Yahya, W. Z. N.; Abu Talip, R. A.; Kurnia, K. A. Prediction of the viscosity of imidazolium-based ionic liquids at different temperatures using the quantitative structure property relationship approach. *New Journal of Chemistry* **2019**, *43*, 16207–16217.

(64) MacQueen, J. B. Some Methods for Classification and Analysis of MultiVariate Observations. Proc. of the fifth Berkeley Symposium on Mathematical Statistics and Probability. 1967; pp 281–297.

(65) Pedregosa, F. et al. Scikit-learn: Machine Learning in Python. *Journal of Machine Learning Research* **2011**, *12*, 2825–2830.

(66) Zheng, W.; Mohammed, A.; Hines, L. G. J.; Xiao, D.; Martinez, O. J.; Bartsch, R. A.; Simon, S. L.; Russina, O.; Triolo, A.; Quitevis, E. L. Effect of Cation Symmetry on the Morphology and Physicochemical Properties of Imidazolium Ionic Liquids. *The Journal of Physical Chemistry B* **2011**, *115*, 6572–6584.

(67) Ignat'ev, N. V.; Barthen, P.; andHelge Willner, A. K.; Sartor, P. A convenient synthesis of triflate anion ionic liquids and their properties. *Molecules* **2012**, *17*, 5319–5338.

(68) Efimova, A.; Hubrig, G.; Schmidt, P. Thermal stability and crystallization behavior of imidazolium halide ionic liquids. *Thermochimica Acta* **2013**, *573*, 162–169.

(69) Seo, K.; Tsay, C.; Hong, B.; Edgar, T. F.; Stadtherr, M. A.; Baldea, M. Rate-Based Process Optimization and Sensitivity Analysis for Ionic-Liquid-Based Post-Combustion Carbon Capture. *ACS Sustainable Chemistry & Engineering* **2020**, *8*, 10242–10258.

(70) Song, D.; Seibert, A. F.; Rochelle, G. T. Mass Transfer Parameters for Packings: Effect of Viscosity. *Industrial & Engineering Chemistry Research* **2018**, *57*, 718–729.

(71) Colburn, A. P. A method of correlating forced convection heat-transfer data and a comparison with fluid friction. *International Journal of Heat and Mass Transfer* **1964**, *7*, 1359–1384.

(72) Lin, Y.-J.; Rochelle, G. T. Optimization of Advanced Flash Stripper for CO_2 Capture Using Piperazine. *Energy Procedia* **2014**, *63*, 1504–1513, 12th International Conference on Greenhouse Gas Control Technologies, GHGT-12.

(73) Lei, Z.; Dai, C.; Chen, B. Gas Solubility in Ionic Liquids. *Chemical Reviews* **2014**, *114*, 1289–1326.

(74) Pereira, L. M.; Martins, V.; Kurnia, K. A.; Oliveira, M. B.; Dias, A. M.; Llovell, F.; Vega, L. F.; Carvalho, P. J.; Coutinho, J. A. High pressure solubility of CH_4, N_2O and N_2 in 1-butyl-3-methylimidazolium dicyanamide: Solubilities, selectivities and soft-SAFT modeling. *The Journal of Supercritical Fluids* **2016**, *110*, 56–64.

(75) Kheirinik, M.; Ahmed, S.; Rahmanian, N. Comparative techno-economic analysis of carbon capture processes: pre-Combustion, post-Combustion, and oxy-Fuel combustion operations. *Sustainability* **2021**, *13*, 13567.

(76) Basha, O. M.; Keller, M. J.; Luebke, D. R.; Resnik, K. P.; Morsi, B. I. Development of a Conceptual Process for Selective CO_2 Capture from Fuel Gas Streams Using [hmim][Tf_2N] Ionic Liquid as a Physical Solvent. *Energy & Fuels* **2013**, *27*, 3905–3917.